

# Formation and Nature of the Active Sites in Bis(imino)pyridine Iron-Based Polymerization Catalysts

Konstantin P. Bryliakov,\* Evgenii P. Talsi, Nina V. Semikolenova, and Vladimir A. Zakharov

Boreskov Institute of Catalysis, Siberian Branch of the Russian Academy of Sciences, 630090, Novosibirsk, Russian Federation

Received November 16, 2008

The activation of 2,6-bis(2,6-diisopropylphenylimino)ethylpyridine iron-based catalysts of ethylene polymerization with methylalumoxane (MAO) and aluminum trialkyls has been studied in detail by  $^1\text{H}$  NMR and EPR spectroscopy. Neutral catalytically active species are formed in  $\text{L}^{\text{IPr}}\text{FeCl}_2/\text{Al}(\text{Alk})_3$  systems. They are complexes  $[\text{L}^{\text{IPr}(-)}\text{Fe}^{(+)}(\mu\text{-Me})_2\text{AlMe}_2]$  (**6**) or  $[\text{L}^{\text{IPr}(-)}\text{Fe}^{(+)}(\mu\text{-iBu})(\mu\text{-X})\text{Al}(\text{iBu})_2]$  (**7** or **8**,  $\text{X} = \text{iBu}$  or  $\text{Cl}$ ), depending on the activator used (either  $\text{AlMe}_3$  or  $\text{Al}(\text{iBu})_3$ ). On the contrary, when “ $\text{AlMe}_3$ -free” methylalumoxane (PMAO) is used as the activator, catalytically active ion pairs of the type  $[\text{LFe}^{\text{II}}(\mu\text{-Me})_2\text{AlMe}_2]^+[\text{MeMAO}]^-$  (**3**) are formed. Intermediates **6** and **8** are relatively unstable and decay within minutes at room temperature, giving rise to an EPR-active iron species with a signal at  $g = 2.08$ , presumably of the type  $\text{L}'\text{Fe}^{\text{I}}\text{—Alk}$  ( $\text{L}'\text{Fe}^{\text{I}}(\mu\text{-Alk})_2\text{Al}(\text{Alk})_2$ ) in the low-spin state  $S = 1/2$  (where  $\text{L}'$  is a modified bis(imino)pyridine ligand). Polymer properties for the different catalyst/activator systems are presented.

## Introduction

Bis(imino)pyridine iron(II) complexes, first introduced as catalysts for ethylene polymerization by Brookhart<sup>1</sup> and Gibson,<sup>2</sup> have attracted substantial interest in the last 10 years. Due to the fruitful structure of the bis(imino)pyridine ligands, allowing a high steric and electronic modularity, the catalysts displayed extremely high ethylene polymerization activities when activated with MAO: up to 20 000 kg PE/mol Fe h bar.<sup>1–3</sup> Later, it was found that bis(imino)pyridine iron catalysts could be activated with aluminum trialkyls ( $\text{AlMe}_3$ ,  $\text{AlEt}_3$ ,  $\text{Al}(\text{iBu})_3$ ,  $\text{Al}(n\text{Hex})_3$ ,  $\text{Al}(n\text{Oct})_3$ ),<sup>4–9</sup> the nature of the activator having been found to affect the molar weight (MW) and molar weight distribution (MWD,  $M_w/M_n$ ) of the resulting polyethylene. In general, activation with MAO led to higher MWs and narrower MWDs.

Since 2001, there has been a discussion concerning the nature of the catalytically active sites in these systems. Talsi et al. employed  $^1\text{H}$  NMR and  $^2\text{H}$  NMR spectroscopy to study

intermediates formed via activation of 2,6-bis(imino)pyridine iron(II) dichloride ( $\text{LFeCl}_2$ ) with MAO,  $\text{AlMe}_3$ ,  $\text{AlMe}_3/\text{B}(\text{C}_6\text{F}_5)_3$ , and  $\text{AlMe}_3/[\text{CPh}_3][\text{B}(\text{C}_6\text{F}_5)_4]$ .<sup>10</sup> The authors suggested that the active components of the  $\text{LFeCl}_2/\text{MAO}$  and  $\text{LFeCl}_2/\text{AlMe}_3$  were the same (neutral) species of the type  $\text{LFe}^{\text{II}}(\text{R})(\mu\text{-Me})_2\text{AlMe}_2$ , where  $\text{R} = \text{Cl}$  or  $\text{Me}$ . On the contrary, Gibson and co-workers, on the basis of EPR and Mössbauer studies, assumed the near 100% conversion of the  $\text{LFeCl}_2$  precursor was into an iron(III) species.<sup>11</sup> In subsequent publications, Talsi and Bryliakov reported the formation of different iron(II) intermediates upon activation of  $\text{LFeCl}_2$  with  $\text{Al}(\text{Alk})_3$  (neutral species  $\text{LFe}^{\text{II}}(\text{R})(\mu\text{-Alk})_2\text{Al}(\text{Alk})_2$ ,  $\text{R} = \text{Cl}$  or  $\text{Alk}$ ) and MAO (ion pairs  $[\text{LFe}^{\text{II}}(\mu\text{-Me})_2\text{AlMe}_2]^+[\text{Me-MAO}]^-$ ).<sup>12,13</sup> Chirik and co-workers isolated cationic complex  $[\text{LFe}^{\text{II}}\text{R}][\text{MeB}(\text{C}_6\text{F}_5)_3]$ , which showed catalytic activity in ethylene polymerization, thus corroborating the viability of iron(II) reactive intermediates.<sup>14</sup>

However, the catalytic behavior of bis(imino)pyridine iron-based systems is rather complicated. From the kinetic studies of Barabanov and co-workers it follows that two types of active sites are present in the systems  $\text{LFeCl}_2/\text{MAO}$  and  $\text{LFeCl}_2/\text{Al}(\text{iBu})_3$ : the more active (and unstable) centers operating at the early stage of polymerization and giving the low-MW polyethylene (PE) are transformed into the less active sites responsible for the higher MW fraction of PE.<sup>15</sup> Kinetic ethylene polymerization data of Kissin support these findings.<sup>16</sup>

In this paper, we report the detailed  $^1\text{H}$  NMR and EPR study of the activation of 2,6-bis(2,6-diisopropylphenylimino)eth-

\* To whom correspondence should be addressed. Fax: +7 383 3308056. E-mail: bryliako@catalysis.ru.

(1) Small, B. L.; Brookhart, M.; Bennet, A. M. *J. Am. Chem. Soc.* **1998**, *120*, 4049.

(2) Britovsek, G. J. P.; Gibson, V. C.; Kimberley, B. S.; Maddox, P. J.; McTavish, S. J.; Solan, G. A.; White, A. J. P.; Williams, D. J. *Chem. Commun.* **1998**, 849.

(3) (a) Britovsek, G. J. P.; Bruce, M.; Gibson, V. C.; Kimberley, B. S.; Maddox, P. J.; Mastroianni, S.; McTavish, S. J.; Redshaw, C.; Solan, G. A.; Stromberg, S.; White, A. J. P.; Williams, D. J. *J. Am. Chem. Soc.* **1999**, *121*, 8728. (b) Gibson, V. C.; Redshaw, C.; Solan, G. A. *Chem. Rev.* **2007**, *107*, 1745.

(4) Kumar, K. R.; Sivaram, S. *Macromol. Chem. Phys.* **2000**, *210*, 1513.

(5) Talsi, E. P.; Babushkin, D. E.; Semikolenova, N. V.; Zudin, V. N.; Zakharov, V. A. *Kinet Catal.* **2001**, *42*, 165.

(6) Semikolenova, N. V.; Zakharov, V. A.; Talsi, E. P.; Babushkin, D. E.; Sobolev, A. P.; Echevskaya, L. G.; Khusniyarov, M. M. *J. Mol. Catal.* **2002**, *182–183*, 283.

(7) Babik, S. T.; Fink, G. J. *Mol. Catal.* **2002**, *188*, 245.

(8) Wang, Q.; Yang, H.; Fan, Z. *Macromol. Rapid Commun.* **2002**, *23*, 639.

(9) Radhakrishnan, K.; Cramail, H.; Deffieux, A.; Francois, P.; Momtaz, A. *Macromol. Rapid Commun.* **2003**, *24*, 251.

(10) Talsi, E. P.; Babushkin, D. E.; Semikolenova, N. V.; Zudin, V. N.; Panchenko, V. N.; Zakharov, V. A. *Macromol. Chem. Phys.* **2001**, *202*, 2046.

(11) Britovsek, G. J. P.; Clensmith, G. K. B.; Gibson, V. C.; Goodgame, D. M. L.; McTavish, S. J.; Pankhurst, Q. A. *Catal. Commun.* **2002**, *3*, 207.

(12) Bryliakov, K. P.; Semikolenova, N. V.; Zudin, V. N.; Zakharov, V. A.; Talsi, E. P. *Catal. Commun.* **2004**, *5*, 45.

(13) Bryliakov, K. P.; Semikolenova, N. V.; Zakharov, V. A.; Talsi, E. P. *Organometallics* **2004**, *23*, 5375.

(14) Boukamp, M. W.; Lobkovsky, E.; Chirik, P. J. *J. Am. Chem. Soc.* **2005**, *127*, 9660.

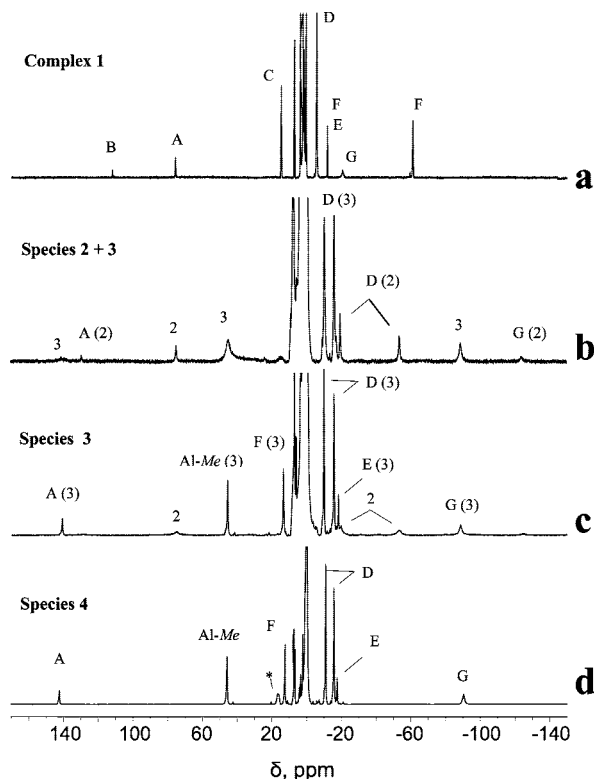


**Figure 1.**  $^1\text{H}$  NMR spectra (toluene- $d_8$ , 296 K) of complex **1** (a) and **1** after the interaction with different activators: (b) PMAO, Al/Fe = 20; (c) PMAO, Al/Fe = 50; (d)  $\text{AlMe}_3/\text{B}(\text{C}_6\text{F}_5)_3$ , Fe:Al:B = 1:15:1.1. Peak assignment corresponds to that in Table 1.

ylpyridine iron(II) catalysts for ethylene polymerization with MAO and trialkylaluminum derivatives, the new data obtained providing a deeper insight into the structure of intermediates formed under the conditions approaching those for real polymerizations. The resulting polymer properties for the different catalyst/activator systems are reported.

## Results and Discussion

**Activation of  $\text{L}^{\text{IPr}}\text{FeCl}_2$  with MAO.** The starting  $\text{L}^{\text{IPr}}\text{FeCl}_2$  complex **1**, when reacted with solid PMAO (polymeric MAO prepared by evacuation of the commercial MAO solution, see Experimental Section) in toluene- $d_8$ , is converted into new iron(II) complexes **2** and **3** having  $^1\text{H}$  NMR spectra with the same range of chemical shifts as **1** (−150 to +150 ppm, Figure 1). Assignment of the NMR resonances of **2** and **3** was done based on the integration of the NMR peaks and comparison of their line widths (the latter correlates with inverse distance from the paramagnetic center).<sup>10,12,13</sup> Unlike the similar  $\text{L}^{\text{Me}}\text{FeCl}_2/\text{MAO}$  system,<sup>10,12,13</sup> in the  $\text{L}^{\text{IPr}}\text{FeCl}_2/\text{MAO}$  system, formation of intermediate complex **2** could only be reliably detected at an Al/Fe ratio of 20, complex **3** becoming the predominating species at higher ratios (Figure 1, Table 1). The use of lower amounts of PMAO (under Al/Fe = 20) was unfruitful, because it did not lead to complete dissolution of iron complex **1** and PMAO. Apparently, it is the methylation with subsequent methyl

abstraction (cationization) resulting in the formation of ion pairs (Scheme 1) which drives the iron complex and PMAO dissolution in this system. This finding is similar to the situation with the metallocene/MAO system where cationization and formation of heterobinuclear ion pairs occurred only at sufficient Al/metal ratios.<sup>17–19</sup> A further increase of the Al/Fe ratio (up to 250), according to  $^1\text{H}$  NMR spectra, does not lead to the appearance of any other bis(imino)pyridine iron species.

To confirm the ionic nature of the intermediates **2** and **3**,  $\text{L}^{\text{IPr}}\text{FeCl}_2$  was activated with  $\text{AlMe}_3/\text{B}(\text{C}_6\text{F}_5)_3$  combination,  $\text{B}(\text{C}_6\text{F}_5)_3$  being known to act via methyl abstraction to generate ion pairs. After combining the reagents at low temperature, the  $^1\text{H}$  NMR spectra of the resulting complex **4** was found to be nearly identical to that of **3**, a single new broad peak at  $\delta$  16.5 (with an integral intensity of 3H) being most likely that of the methyl group of the  $[\text{CH}_3\text{B}(\text{C}_6\text{F}_5)_3]^-$  counteranion (Figure 1, Table 1).

Species **2–4** persist in solution for hours at room temperature. However, their concentration decreased with time (this decay accompanied by a color change from initial light brown to dark brown), and finally, precipitation of a dark solid in the NMR tube occurred. In line with the decay of the concentration of **2–4**, the appearance of some new EPR-active ( $g = 2.08$ ,  $\nu\Delta_{1/2} = 330$  G) iron species was detected (Figure 2). In a separate experiment, it was found that a similar  $^1\text{H}$  NMR spectrum decay along with the appearance of the EPR signal at  $g = 2.08$  was the case for the 2,6-dimethyl analog of **1**:  $\text{L}^{\text{Me}}\text{FeCl}_2$ . The latter is less prone to conversion to EPR-active Fe species: a detectable feature at  $g = 2.08$  was observed only in 2.0–2.5 h after the activation of  $\text{L}^{\text{Me}}\text{FeCl}_2$  with PMAO (Al/Fe = 100).

EPR spectra of this type were detected by Gibson and co-workers and assigned to iron(III) species.<sup>11</sup> The authors identified their species based on the observed Mössbauer data ( $\delta + 0.16$  mm s $^{-1}$ ,  $E\Delta_Q$  0.58 mm s $^{-1}$ ) falling in the range typical for high-spin iron(III) species.

However, formation of iron(III) from the iron(II) precursors under the reductive conditions (MAO containing  $\text{AlMe}_3$ ) is unfeasible. On the contrary, it is very likely that the EPR spectra reported in ref 11 as well as those presented in Figure 2 can belong to a low-spin ( $S = 1/2$ ) iron(I) complex<sup>22</sup> (for such complexes, the typical  $g$  factors are 2.0–2.2).<sup>23–27</sup> The nature of these species will be discussed further.

**Activation of  $\text{L}^{\text{IPr}}\text{FeCl}_2$  with  $\text{AlMe}_3$ .** The interaction of the 2,6-dimethyl analog of **1** ( $\text{L}^{\text{Me}}\text{FeCl}_2$ ) with  $\text{AlMe}_3$  was studied previously;<sup>13</sup> the authors concluded that the resulting intermedi-

(17) Babushkin, D. E.; Semikolenova, N. V.; Zakharov, V. A.; Talsi, E. P. *Macromol. Chem. Phys.* **2000**, *201*, 558.

(18) Babushkin, D. E.; Brintzinger, H. H. *J. Am. Chem. Soc.* **2002**, *124*, 12869.

(19) Bryliakov, K. P.; Talsi, E. P.; Bochmann, M. *Organometallics* **2004**, *23*, 149.

(20) Bochmann, M.; Lancaster, S. *Angew. Chem., Int. Ed. Engl.* **1994**, *17*, 1634.

(21) Brintzinger, H. H.; Fischer, D.; Mulhaupt, R.; Rieger, B.; Waymouth, R. M. *Angew. Chem., Int. Ed. Engl.* **1995**, *34*, 1143.

(22) The Mössbauer parameters for iron(I) complexes are rather scarce in the literature, which would not allow the unambiguous assignment of Gibson's data.<sup>11</sup>

(23) Kuska, H. A.; Rogers, M. T. *Electron spin resonance of first row transition metal complex ions*; Interscience Publishers: New York, 1968.

(24) Cohen, I. A.; Ostfeld, D.; Lichtenstein, B. *J. Am. Chem. Soc.* **1972**, *94*, 4522.

(25) Srivatsa, G. S.; Sawyer, D. T.; Boldt, N. J.; Bocian, D. F. *Inorg. Chem.* **1985**, *24*, 2123.

(26) Kim, S. H.; Yang, T. C.; Perera, R.; Jin, S.; Bryson, T. A.; Sono, M.; Davydov, R.; Dawson, J. H.; Hoffman, B. M. *Dalton Trans.* **2005**, *21*, 3464.

(27) Davydov, R.; Hoffman, B. M. *J. Biol. Inorg. Chem.* **2008**, *13*, 357.

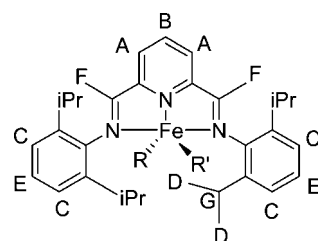
(15) (a) Barabanov, A. A.; Zakharov, V. A.; Semikolenova, N. V.; Echevskaja, L. G.; Matsko, M. A. *Macromol. Chem. Phys.* **2005**, *206*, 2292. (b) Barabanov, A. A.; Bukatov, G. D.; Zakharov, V. A.; Semikolenova, N. V.; Mikenas, T. B.; Echevskaja, L. G.; Matsko, M. A. *Macromol. Chem. Phys.* **2006**, *207*, 1368.

(16) Kissin, Y. V.; Qian, C.; Xie, G.; Chen, Y. *J. Polym. Sci., Part A: Polym. Chem.* **2006**, *44*, 6159.

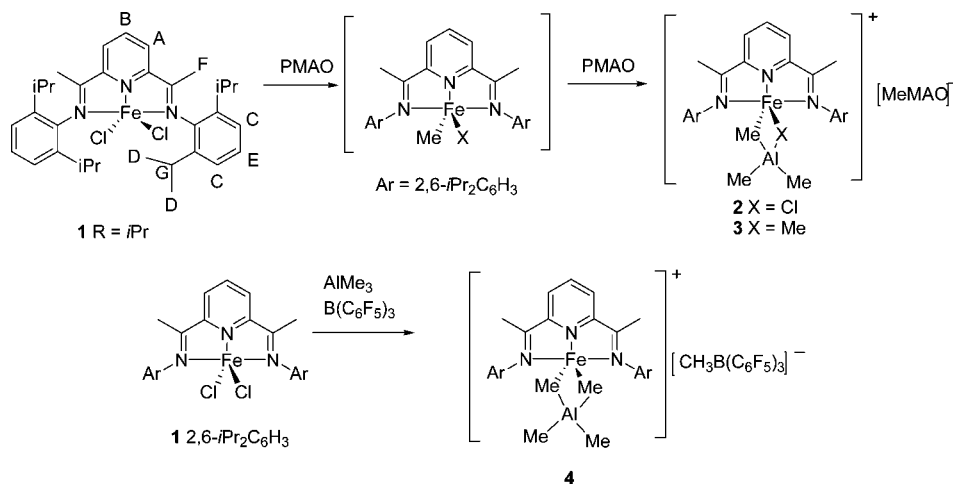
Table 1.  $^1\text{H}$  NMR Data for the Complexes Considered (toluene- $d_8$ :  $\delta$ , ppm ( $\nu\Delta_{1/2}$ , Hz))<sup>a</sup>

complex	T, K	A Py- $H_m$	B Py- $H_p$	C Ar- $H_m$	D ArCH(Me) <sub>2</sub>	E Ar- $H_p$	F N=C(Me)	G ArCH(Me) <sub>2</sub>	X	Y	Z
<b>1</b>	296	75.6 (80)	111.8 (90)	14.6 (30)	-5.7 (85) -5.9 (40)	-11.8 (30)	-61.0 (80)	-20.8 (400)			
<b>2<sup>b</sup></b>	296	128.8 (280)	NA	NA	-19.7 (200) -53.8 (344)	NA	NA	-124 (780)	NA		
<b>3<sup>c</sup></b>	263	171.0 (940)	NA	NA	-13.8 (260) -20.5 (430)	-23.7 (150)	12.8 (340)	-119.0 (2000)	60.0 <sup>d</sup> (620)		
<b>3<sup>c</sup></b>	296	140.6 (190)	NF	NF	-9.9 (95) -15.6 (130)	-18.2 (100)	13.4 (140)	-88.6 (730)	45.6 <sup>d</sup> (170)		
<b>4<sup>e</sup></b>	263	170.9 (360)	NF	NF	-15.3 (115) -20.3 (160)	-22.6 (90)	11.0 (160)	-119.5 (850)	59.0 <sup>d</sup> (270)		
<b>4<sup>e</sup></b>	296	142.2 (215)	NF	NF	-11.2 (110) -15.8 (140)	-17.7 (100)	12.4 (120)	-90.5 (530)	45.7 <sup>d</sup> (180)		
<b>5<sup>f</sup></b>	263	116.2 (320)	422 (470)	NF	-15.9 (170) -20.5 (180)	-17.1 (190)	-287.7 (600)	-105.0 (700)	44.6 <sup>d</sup> (220)		
<b>5<sup>f</sup></b>	296	99.3 (370)	370.6 (730)	NF	-13.1 (180) -17.3 (190)	-13.9 (150)	-249.1 (660)	-86.8 (750)	37.4 <sup>d</sup> (260)		
<b>6<sup>g</sup></b>	253	70.3 (250)	432.9 (750)	9.5 (260)	-1.6 -7.8 (240)	-10.9 (150)	-267.4 (650)	NA	25.6 <sup>d</sup> (350)		
<b>6</b>	263	66.0 (260)	409.8 (170)	9.2 (340)	-1.5 (300) -7.2 (310)	-9.9 (190)	-252.1 (500)	NA	23.9 <sup>d</sup> (370)		
<b>L<sup>iPr</sup>FeCl</b>	263	77.4 (240)	442.0 (700)	-8.9 (70)	-25.8 (90) -40.2 (260)	-16.6 (60)	-243.0 (470)	-133.0 (820)			
<b>7<sup>h</sup></b>	263	115.6 (700)	431.0 (1200)	NF	-16.7 (100) -21.3 (130)	NF	-289.4 (940)	-107.8 (1100)	47.4 <sup>h</sup> (700)	NA	20.0 <sup>h</sup> (220)
<b>7<sup>h</sup></b>	296	97.3 (95)	373.8 (390)	NF	-13.4 (100) -17.8 (130)	NF	-248.3 (350)	-88.2 (590)	39.1 <sup>h</sup> (250)	28.2 <sup>h</sup> (125)	16.7 <sup>h</sup> (70)
<b>8</b>	263	68.0 (190)	357.9 (480)	-6.2 (80)	-16.7 (95) -28.9 (160)	-15.1 (110)	-195.7 (260)	-105.6 (550)	92.2 <sup>h</sup> (420)	43.4 <sup>h</sup> (200)	25.2 <sup>h</sup> (130)
<b>8<sup>i</sup></b>	296	61.5 (95)	321.9 (500)	-3.9 (100)	-13.0 (100) -24.8 (180)	-12.9 (130)	-178.1 (370)	-86.2 (630)	79.6 <sup>h</sup> (490)	36.0 <sup>h</sup> (135)	21.2 <sup>h</sup> (190)
<b>L<sup>iPr</sup>FeCl</b>	296	67.3 (150)	381.7 (250)	-6.0 (40)	-22.8 (70) -33.2 (160)	-13.1 (40)	-211.0 (200)	-108.2 (440)			
<b>L<sup>iPr</sup>FeMe<sup>j</sup></b>	296	59.6 (90)	211.2 (180)	-2.3 (50)	-11.5 (65) -20.9 (130)	NA	-164.8 (220)	-71.6 (340)			

<sup>a</sup> NF, not found. NA, not reliably assigned. Ligand protons labeling scheme: R, R' = Cl, Me, *i*Bu.



<sup>b</sup> In the system **1**/PMAO = 20. <sup>c</sup> In the system **1**/PMAO = 50. <sup>d</sup> X stands for Al(CH<sub>3</sub>)<sub>2</sub>. <sup>e</sup> In the system **1**/AlMe<sub>3</sub>/B(C<sub>6</sub>F<sub>5</sub>)<sub>3</sub> = 1:15:1.1, an additional broad peak assigned to [CH<sub>3</sub>B(C<sub>6</sub>F<sub>5</sub>)<sub>3</sub>]<sup>-</sup> is found at  $\delta$  16.5 (296 K) and 20.7 (263 K). <sup>f</sup> In the system **1**/AlMe<sub>3</sub> = 10. <sup>g</sup> In the system **1**/AlMe<sub>3</sub> = 10. <sup>h</sup> In the system **1**/Al(*i*Bu)<sub>3</sub> = 30, X stands for Al-CH<sub>2</sub>-, Y for Al-CH<sub>2</sub>-CH-, and Z for Al-CH<sub>2</sub>CH(CH<sub>3</sub>)<sub>2</sub> peaks. <sup>i</sup> In the system **1**/Al(*i*Bu)<sub>3</sub> = 30, X stands for Al-CH<sub>2</sub>-, Y for Al-CH<sub>2</sub>-CH-, and Z for Al-CH<sub>2</sub>CH(CH<sub>3</sub>)<sub>2</sub> peaks.

Scheme 1. Interaction of **1** with MAO and AlMe<sub>3</sub>/B(C<sub>6</sub>F<sub>5</sub>)<sub>3</sub>

ates were neutral species of the type [LFe<sup>II</sup>(R)( $\mu$ -Alk)<sub>2</sub>Al(Alk)<sub>2</sub>] (R = Cl or Me), the unexpectedly large paramagnetic shifts of this species (up to 358 and -276 ppm) being left without explanation. Since the time of publication,<sup>13</sup> the chemistry of bis(imino)pyridine iron complexes greatly advanced: in particular, the ability of the tridentate ligand to accept one or even two electrons upon the complex reduction with various agents was well documented.<sup>28–33</sup> It could be expected that the reaction of **1** with aluminum alkyls would result in the reduction of the former; however, the electron would be accepted by the tridentate ligand rather than the iron center, leaving iron in the +2 oxidation state.

To explore this hypothesis, **1** was reacted with AlMe<sub>3</sub> at low temperature to yield species **5** (Figure 3a). The range of its  $^1\text{H}$  NMR shifts (+430 to -300 ppm) is much higher than for the starting **1** and close to that for the previously reported L<sup>iPr</sup>FeCl (Figure 3b).<sup>29,33</sup> In the latter, iron retains the 2+ oxidation state,

(29) Bouwkamp, M. W.; Bart, S. C.; Hawrelak, E. J.; Trovitch, R. J.; Lobkovsky, E.; Chirik, P. J. *Chem. Commun.* **2005**, 3406.

(30) Bart, S. C.; Lobkovsky, E.; Bill, E.; Wiegardt, K.; Chirik, P. J. *Inorg. Chem.* **2007**, *46*, 7055.

(31) Trovitch, R. J.; Lobkovsky, E.; Bill, E.; Chirik, P. J. *Organometallics* **2008**, *27*, 1470.

(32) Bart, S. C.; Chlopek, K.; Bill, E.; Bouwkamp, M. W.; Lobkovsky, E.; Neese, F.; Wiegardt, K.; Chirik, P. J. *J. Am. Chem. Soc.* **2006**, *128*, 13901.

(33) Fernández, I.; Trovitch, R. J.; Lobkovsky, E.; Chirik, P. J. *Organometallics* **2008**, *27*, 109.

(28) Bart, S. C.; Lobkovsky, E.; Chirik, P. J. *J. Am. Chem. Soc.* **2004**, *126*, 13794.

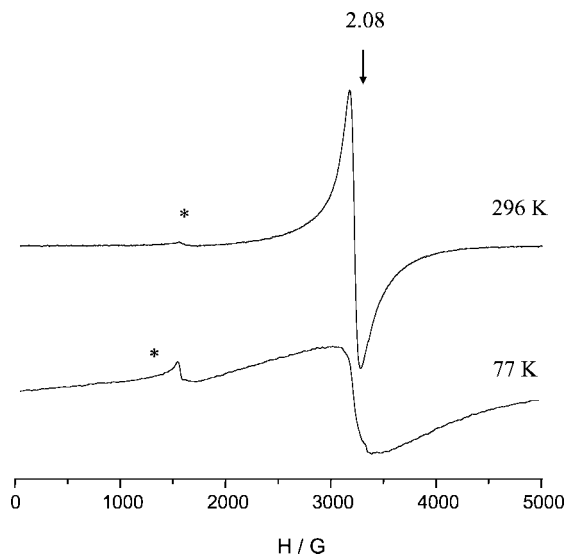


**Figure 2.** EPR spectra measured after the interaction (10 min) of **1** with PMAO (Al/Fe = 20). Asterisks mark  $\text{Fe}^{3+}$  impurities in the NMR tube glass.

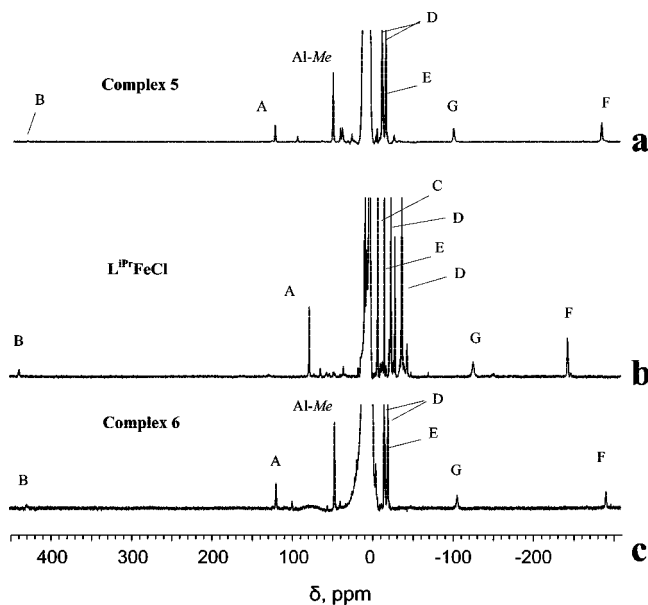


**Figure 3.**  $^1\text{H}$  NMR spectra (toluene- $d_8$ , 263 K) of (a) **1**/AlMe $_3$  (Al/Fe = 10), (b) complex  $\text{L}^{\text{iPr}}\text{FeCl}$ , and (c)  $\text{L}^{\text{iPr}}\text{FeCl}/\text{AlMe}_3$  (Al/Fe = 10).

one electron being distributed over the tridentate ligand, to yield a complex of the type  $\text{L}^{\text{iPr}(-)}\text{Fe}^{(+)}\text{Cl}$ .<sup>32</sup> It has  $\mu_{\text{eff}} = 3.5 \mu\text{B}$ , indicative of the high-spin  $\text{Fe}(\text{II})$  ion ( $S_{\text{Fe}} = 2$ ) coupled antiferromagnetically to a ligand radical ( $S_{\text{L}} = 1/2$ ).<sup>32</sup> The unpaired electron spin density on the pyridine part of the ligand (with respect to the starting **1**) leads to the increased paramagnetic shifts in the  $^1\text{H}$  NMR spectra of such species.

Apparently, the interaction of **1** with AlMe $_3$  results in one-electron reduction of the former (to yield species **5**), as it is seen from the high paramagnetic shifts of the  $^1\text{H}$  NMR peaks at  $\delta$  422 (Py- $H_p$ ) and  $-288$  (N=C(Me)) at 263 K (Table 1); furthermore, the new peak at  $\delta$  45.5 with an integral intensity of 6H evidence the presence of Al(CH $_3$ ) $_2$  moieties in the structure of **5**. In line with this picture, reaction of  $\text{L}^{\text{iPr}}\text{FeCl}$  with AlMe $_3$  led to the same species **5** (Figure 3c). One can conclude that **5** is a heterobinuclear complex  $[\text{L}^{\text{iPr}(-)}\text{Fe}^{(+)}(\mu\text{-X})(\mu\text{-Me})\text{AlMe}_2]$ , where X = Cl or Me. To establish the nature of

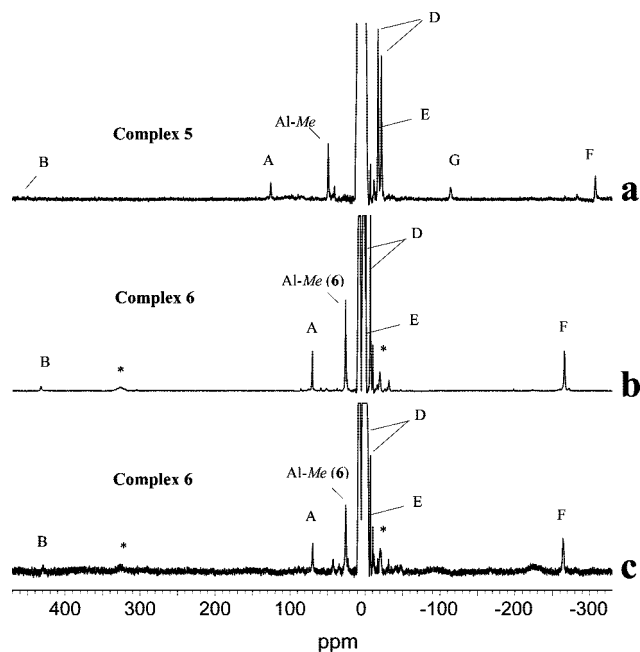


**Figure 4.**  $^1\text{H}$  NMR spectra (toluene- $d_8$ , 253 K) of (a)  $\text{L}^{\text{iPr}}\text{FeCl}/\text{AlMe}_3$  (Al/Fe = 5), (b)  $\text{L}^{\text{iPr}}\text{FeMe}/\text{AlMe}_3$  (Al/Fe = 10), and (c)  $\text{L}^{\text{iPr}}\text{FeCl}/\text{AlMe}_3$  (Al/Fe = 30). Asterisks mark peaks that were not reliably assigned.

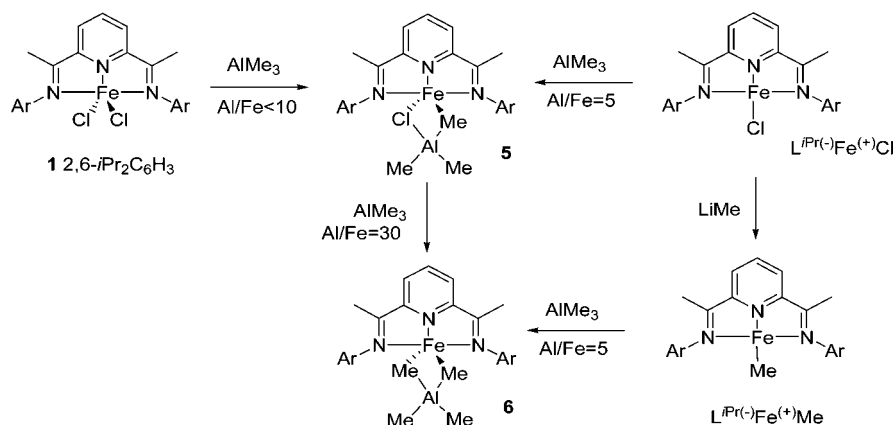
the bridging ligands, we prepared  $\text{L}^{\text{iPr}}\text{FeMe}$  complex and reacted it with AlMe $_3$ . The  $^1\text{H}$  NMR spectrum of the resulting species **6** differed from that of **5** (cf. Figure 4a and 4b). As soon as the starting complex  $\text{L}^{\text{iPr}}\text{FeMe}$  contained no chloride ligands, apparently, **6** could be identified as dimethyl-bridged heterobinuclear species  $[\text{L}^{\text{iPr}(-)}\text{Fe}^{(+)}(\mu\text{-Me})_2\text{AlMe}_2]$ . Species **6** was obtained in the system  $\text{L}^{\text{iPr}}\text{FeCl}/\text{AlMe}_3$  at the Al/Fe ratio of 30 (Figure 4b and 4c). Thus, for the systems with AlMe $_3$ , the following reaction scheme can be adopted (Scheme 2).

The use of low temperatures (253–263 K) was dictated by the instability of the iron complexes **5** and **6** in the presence of AlMe $_3$ . At room temperature,  $^1\text{H}$  NMR spectra of **5** and **6** disappeared within minutes. This is in contrast to the  $\text{L}^{\text{Me}}\text{FeCl}_2/\text{AlMe}_3$  (Al/Fe = 15–30) system where such intermediates could still be observed after storing the system for hours at room temperature.<sup>13</sup> On the basis of the new data, we can define more exactly the structure of intermediates formed in  $\text{L}^{\text{Me}}\text{FeCl}_2/\text{AlR}_3$  systems.<sup>12,13</sup> Apparently, the intermediates previously assigned to  $[\text{L}^{\text{Me}}\text{Fe}^{\text{II}}(\text{R})(\mu\text{-Alk})_2\text{Al}(\text{Alk})_2]$  (R = Cl or Me) species<sup>13</sup> are actually alkyl-bridged heterobinuclear species  $[\text{L}^{\text{Me}(-)}\text{Fe}^{(+)}(\mu\text{-Alk})_2\text{Al}(\text{Alk})_2]$ .

To disclose the ways of the intermediates **5** and **6** degradation, the interaction of **1**,  $\text{L}^{\text{iPr}}\text{FeCl}$ , and  $\text{L}^{\text{iPr}}\text{FeMe}$  with AlMe $_3$  was monitored by EPR (the starting complexes **1**,  $\text{L}^{\text{iPr}}\text{FeCl}$ , and  $\text{L}^{\text{iPr}}\text{FeMe}$  are EPR inactive). In all cases, a similar picture was observed. At the first stage, a narrow signal at  $g = 2.003$  appeared followed by a new broad peak at  $g = 2.08$  (Figure 5). The former peak belongs to the  $[\text{L}^{\text{iPr}(-)}\text{Al}^{(+)}\text{Me}_2]$  complex discovered by Gambarotta and co-workers (formed upon extrusion of iron from the structure of the bis(imino)pyridine complex).<sup>34</sup> The same spectrum at  $g = 2.003$  can be observed upon reacting the bis(imino)pyridine ligand,  $\text{L}^{\text{iPr}}$ , with AlMe $_3$  (see insert for Figure 5a).

The nature of the species formed in the presence of AlMe $_3$  and MAO with the broad EPR spectra at  $g = 2.08$  is not that clear. Apparently, modification of the bis(imino)pyridine ligand can take place in the presence of AlMe $_3$  or MAO (see ref 35



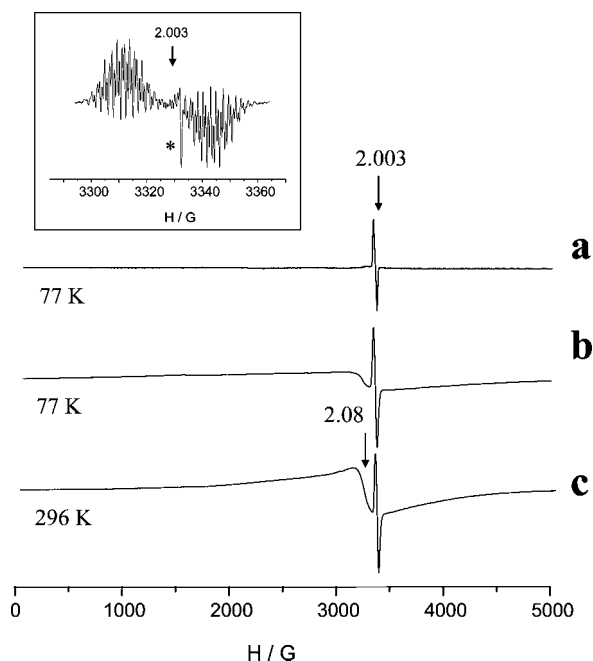
Scheme 2. Interaction of Bis(imino)pyridine Iron Complexes with AlMe<sub>3</sub>

and references therein) to give species of the type  $L'Fe^I-Alk$  (as  $L'Fe^I(\mu-Alk)_2Al(Alk)_2$  adduct, where  $L'$  is a modified bis(imino)pyridine ligand) with a singlet ground spin state. The formation of iron(I) species in an iron-based catalytic system for ethylene polymerization is neither unexpected nor new: a set of active  $S = 1/2$  iron(I) complexes has been reported in the Ziegler-type catalytic system  $Fe(acac)_3$  + diphenylphosphinoethane +  $AlEt_3$ , displaying EPR spectra at  $g_{iso} = 2.07-2.10$ .<sup>36</sup>

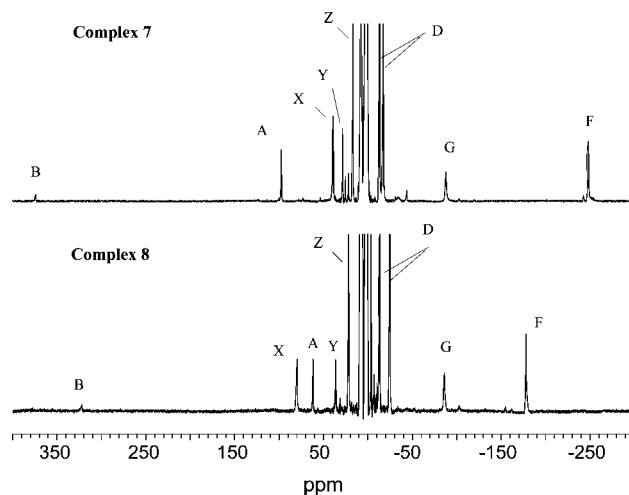
**Activation of  $L^{iPr}FeCl_2$  with  $Al(iBu)_3$ .** The interaction of **1** with  $Al(iBu)_3$  ( $Al/Fe = 10-30$ ) yielded heterobinuclear species **7** similar to **5** (according to their  $^1H$  NMR spectra, Figure 6a). In contrast to **5**, complex **7** was stable for days at room temperature, although the EPR measurements indicated the presence of small quantities of both EPR-active species with peaks at  $g = 2.003$  and  $2.08$ . This may be caused by the lower reactivity of  $Al(iBu)_3$  (compared to  $AlMe_3$ ) toward the bis(imino)pyridine ligand alkylation. The interaction of  $L^{iPr}FeCl$  or  $L^{iPr}FeMe$  with  $Al(iBu)_3$ , however, was found to yield species **8**

with a  $^1H$  NMR spectrum somewhat different from those of **7**. By analogy with the system **1**/ $AlMe_3$ , complexes **7** and **8** were assigned to  $[L^{iPr(-)}Fe^{(+)}(\mu-Cl)(\mu-iBu)Al(iBu)_2]$  and  $[L^{iPr(-)}Fe^{(+)}(\mu-iBu)_2Al(iBu)_2]$ , respectively. **8** was found to decompose at room temperature within 10–15 min in the system  $L^{iPr}FeMe/Al(iBu)_3$  and 2–3 min in the system  $L^{iPr}FeCl/Al(iBu)_3$ .<sup>37</sup> The EPR spectra indicated the appearance of the spectrum of  $[L^{iPr(-)}Al^{(+)}Me_2]$  at  $g = 2.003$ . Scheme 3 represents the reactions taking place in these systems. Unlike the formation of dialkyl-bridged complex  $[L^{iPr(-)}Fe^{(+)}(\mu-Me)_2AlMe_2]$  (**6**) in the system **1**/ $AlMe_3$ , complex **7** formed in the system **1**/ $Al(iBu)_3$  did not convert to **8** even at the relatively high  $Al/Fe$  ratio of 30. Apparently, higher  $Al/Fe$  ratios are required for the formation of **8** (that is usually the case in conditions of practical polymerizations).

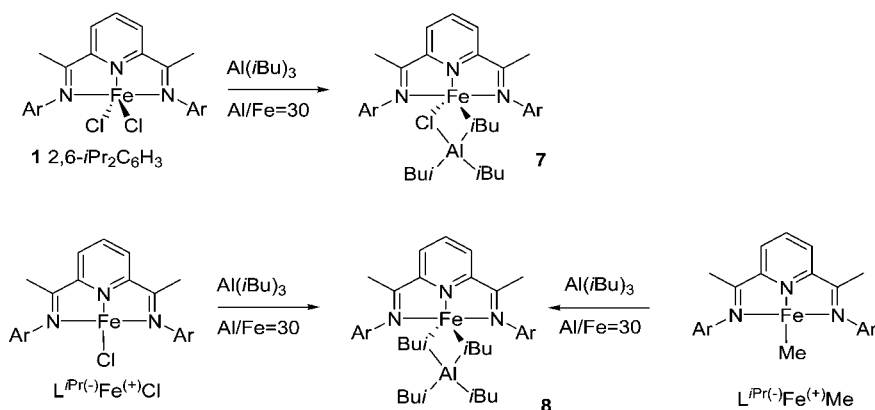
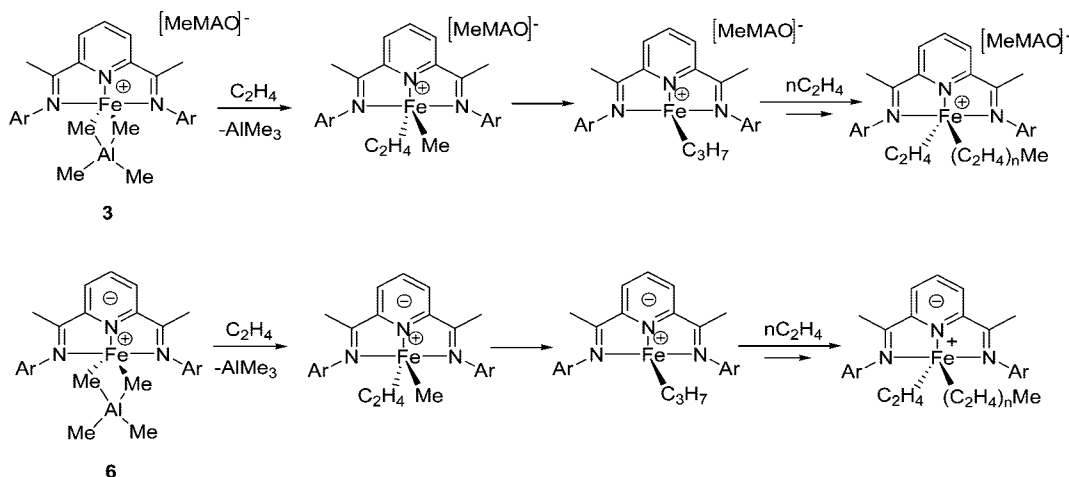
**Formation of the Active Sites for Ethylene Polymerization.** On the basis of the data presented in the previous sections, one can conclude that, depending on the activator used, three types of active sites or active sites precursors can be present in the catalytic systems based on the  $L^{iPr}FeCl_2$  catalyst **1** in conditions close to practical polymerization. They are (1) ion pairs  $[L^{iPr}Fe^{II}(\mu-Me)_2AlMe_2]^+[MeMAO]^-$  (**3**) in the system **1**/MAO, (2) electroneutral heterobinuclear complexes  $[L^{iPr(-)}Fe^{(+)}(\mu-Me)_2AlMe_2]$  (**6**) in the system **1**/ $AlMe_3$ , and (3) electroneutral heterobinuclear complexes  $[L^{iPr(-)}Fe^{(+)}(\mu-iBu)(\mu-X)Al(iBu)_2]$  (**7** or **8**,  $X = iBu$  or  $Cl$ ) in the system **1**/ $Al(iBu)_3$ . The reason why nominally neutral complexes **6–8** can catalyze olefin polymerization is



**Figure 5.** EPR spectra measured after the interaction of  $L^{iPr}FeCl$  with  $AlMe_3$  ( $Al/Fe = 3$ ): (a) after mixing the reagents at low temperature ( $-40$  °C), (b) after warming the previous sample to room temperature, and (c) the same sample stored at room temperature for 1 h. Insert for Figure 1a: EPR spectrum (296 K) of the mixture of  $AlMe_3/L^{iPr}$  (asterisk marks an impurity in the sample tube).



**Figure 6.**  $^1H$  NMR spectra (toluene- $d_8$ , 296 K) of (a)  $L^{iPr}FeCl_2/Al(iBu)_3$  ( $Al/Fe = 30$ ) and (b)  $L^{iPr}FeMe/Al(iBu)_3$  ( $Al/Fe = 30$ ). X stands for  $Al-CH_2-$ , Y for  $Al-CH_2-CH-$ , and Z for  $Al-CH_2CH(CH_3)_2$  peaks.

Scheme 3. Interaction of Bis(imino)pyridine Iron Complexes with Al(*i*Bu)<sub>3</sub>Scheme 4. Polymerization Initiation and Propagation in the Systems 1/MAO and 1/AlMe<sub>3</sub>Table 2. Ethylene Polymerization over Bis(imino)pyridine Iron Complexes<sup>a</sup>

entry	complex	cocatalyst	Al/Fe	PE yield (g)	PE yield (kg PE/mol Fe atm)	$M_n \times 10^{-3}$	$M_w \times 10^{-3}$	$M_z \times 10^{-3}$	$M_w/M_n$	$M_z/M_w$
1	$L^{iPr}FeCl_2$ (1)	MAO	500	18.5	1850	11	220	2400	20.0	10.9
2	$L^{iPr}FeCl_2$ (1)	AlMe <sub>3</sub>	100	20.9	2090	14	150	2000	10.7	13.3
3	$L^{iPr}FeCl_2$ (1)	PMAO (20)	500	16.2	1620	24	230	2600	9.6	11.3
4	$L^{iPr}FeCl_2$ (1)	Al( <i>i</i> Bu) <sub>3</sub>	100	20.3	1000 <sup>b</sup>	11	56	180	5.1	3.2
5	$L^{iPr}FeCl_2$	Al( <i>i</i> Bu) <sub>3</sub>	500	10.3	1030	22	110	390	5.0	3.5
6	$L^{iPr}FeCl$	MAO	500	17.8	1780	13	290	3500	22.3	12.1
7	$L^{iPr}FeCl$	AlMe <sub>3</sub>	100	14.9	1490	14	270	2500	19.3	9.3
8	$L^{iPr}FeMe$	MAO	500	11.5	1150	20	240	2900	12.0	12.1
9	$>L^{iPr}FeMe$	AlMe <sub>3</sub>	100	15.6	1560	15	170	1500	11.3	8.8
10	$L^{iPr}FeMe$	Al( <i>i</i> Bu) <sub>3</sub>	100	10.1	1010	32	100	270	3.1	2.7

<sup>a</sup> Polymerization conditions:  $2 \times 10^{-6}$  mol of the catalyst, toluene (100 mL) solution of the co-catalyst, 5 atm ethylene pressure, 35 °C, polymerization time 20 min. <sup>b</sup> Ethylene pressure 10 atm.

explained by the peculiarity of their structure which implies the positive charge on the Fe<sup>(II)</sup> center and one electron distributed over the iminopyridine ligand. Thus, the polymerization process can be schematically represented as in Scheme 4.

**Ethylene Polymerization over Bis(imino)pyridine Iron Complexes.** To confront the nature of active sites with the catalytic performance of bis(imino)pyridine iron complexes, ethylene polymerization experiments with different cocatalysts

were performed (Table 2). The use of commercial MAO (entries 1, 6, and 8) led to formation of PE with the widest MWDs. The most likely reason for this is the presence of AlMe<sub>3</sub> in the commercial MAO (up to 30% mol) which can (1) result in the formation of multiple active sites (of the type 3 and 6) upon activation of 1 with AlMe<sub>3</sub> and MAO and (2) cause enhanced chain transfer. Indeed, when AlMe<sub>3</sub> and PMAO(20) (polymeric MAO evacuated at 20 °C, see Experimental Section) were used as cocatalysts separately for the activation of 1, polymers with

(34) Scott, J.; Gambarotta, S.; Korobkov, I.; Knijnenburg, Q.; de Bruin, B.; Budzelaar, P. H. M. *J. Am. Chem. Soc.* **2005**, *127*, 17204.

(35) Scott, J.; Gambarotta, S.; Korobkov, I.; Budzelaar, P. H. *J. Am. Chem. Soc.* **2005**, *127*, 13019.

(36) Saraev, V. V.; Schmidt, F. K.; Gruznykh, V. A.; Bakunina, T. I.; Mironova, L. V. *Koord. Khim.* **1979**, *5*, 1472.

(37) The difference in stability is not clear. One could expect that species formed in the systems  $L^{iPr}FeCl/Al(iBu)_3$  and  $L^{iPr}FeMe/Al(iBu)_3$  differ in the nature of the bridging ligands:  $[L^{iPr(-)}Fe^{(+)}(\mu-iBu)_2Al(iBu)_2]$  and  $[L^{iPr(-)}Fe^{(+)}(\mu-Me)(\mu-iBu)Al(iBu)_2]$ , respectively, which could be hardly distinguishable by <sup>1</sup>H NMR. This might explain their different stabilities and catalytic activities (see the text).

lower MWDs (ca. 10) were obtained (entries 2 and 3), polymer obtained with PMAO(20) displaying almost two times higher average  $M_n$ .

$^1\text{H}$  NMR spectra of the system **1**/commercial MAO (Al/Fe = 200) indicated the presence of species **3**. Apparently, electroneutral complexes **6** (formed via reduction of **1** with  $\text{AlMe}_3$  present in MAO) could not be detected because of the formation of labile adducts with MAO (of the type  $\mathbf{6} + \text{MAO} \leftrightarrow \mathbf{6} \cdot \text{MAO}$ ) and hence MAO-induced nonuniform line broadening. For the  $\text{L}^{\text{iPr}}\text{FeCl}$ /commercial MAO (Al/Fe = 200) sample (expected to yield species **6** via interaction with  $\text{AlMe}_3$ ), no  $^1\text{H}$  NMR spectra were observed in the temperature range 253–296 K, due to the line broadening caused by complexation with MAO.

When  $\text{Al}(i\text{Bu})_3$  was used as the cocatalyst for **1**, PEs with much more narrow MWDs were obtained (Table 2, entries 4 and 5). Interestingly, the increase of the Al/Fe ratio from 100 to 500 resulted in the 2-fold increase of  $M_n$ , while the MWD and activity remained unchanged.

The activation of  $\text{L}^{\text{iPr}}\text{FeCl}$  with commercial MAO and  $\text{AlMe}_3$  gave predictably similar polymerization results, confirming the role of  $\text{AlMe}_3$  as the true activator in both cases (entries 6 and 7). Apparently, this is accounted for by the formation of the same active species **6**.  $\text{Al}(i\text{Bu})_3$  appeared to be a poor activator for  $\text{L}^{\text{iPr}}\text{FeCl}$  (no PE formed at Al/Fe = 100 and only 140 kg PE/mol Fe atm at Al/Fe = 500, data not shown). The reason for this is unclear.

$\text{L}^{\text{iPr}}\text{FeMe}$ , when activated with commercial MAO and  $\text{AlMe}_3$ , displayed close catalytic activities and gave polymers with similar properties (entries 8 and 9). When  $\text{Al}(i\text{Bu})_3$  was used for the activation of  $\text{L}^{\text{iPr}}\text{FeMe}$ , PE with the narrowest MWD formed ( $M_w/M_n = 3.1$ ). However, in none of these cases the catalytic systems can be regarded as single-site ones, corroborating the conclusion of Barabanov<sup>15</sup> and Kissin<sup>16</sup> that active sites transformation may be the case during the polymerization process catalyzed by bis(imino)pyridine iron catalysts.

## Conclusions

We can conclude that neutral active species or their precursors are formed in  $\text{L}^{\text{iPr}}\text{FeCl}_2/\text{Al}(\text{Alk})_3$  catalytic systems. They are complexes  $[\text{L}^{\text{iPr}(-)}\text{Fe}^{(+)}(\mu\text{-Me})_2\text{AlMe}_2]$  (**6**) or  $[\text{L}^{\text{iPr}(-)}\text{Fe}^{(+)}(\mu\text{-}i\text{Bu})(\mu\text{-X})\text{Al}(i\text{Bu})_2]$  (**7** or **8**, X =  $i\text{Bu}$  or Cl), depending on the activator used (either  $\text{AlMe}_3$  or  $\text{Al}(i\text{Bu})_3$ ). On the contrary, when “ $\text{AlMe}_3$ -free” methylalumoxane (PMAO) is used as the activator, ion pairs of the type  $[\text{L}^{\text{iPr}}\text{Fe}^{\text{II}}(\mu\text{-Me})_2\text{AlMe}_2]^+[\text{MeMAO}]^-$  (**3**) are formed. Intermediates **6** and **8** are relatively unstable at room temperature and decay within minutes at room temperature. At the same time, formation of new EPR-active species is observed: (1)  $\text{L}^{\text{iPr}}\text{AlMe}_2$  having signal at  $g = 2.003$  and (2) another species (signal at  $g = 2.08$ ), presumably of the type  $\text{L}'\text{Fe}^{\text{I}}\text{-Alk}$  ( $\text{L}'\text{Fe}^{\text{I}}(\mu\text{-Alk})_2\text{Al}(\text{Alk})_2$ ) in the low-spin state  $S = 1/2$  (where  $\text{L}'$  is a modified bis(imino)pyridine ligand). Ion-pair intermediates **3** are more stable and persist in solution for hours; however, formation of EPR signals at  $g = 2.08$  was also observed in the systems with PMAO as the activator.

It is generally accepted that metallocene and postmetallocene catalysts must be activated with cationizing cocatalysts for the ion-pair active sites to form. However, it is not necessarily the case for bis(imino)pyridine iron complexes: when activated with aluminum trialkyls, they yield iron(II) species of the type  $[\text{L}^{\text{iPr}(-)}\text{Fe}^{(+)}(\mu\text{-Alk})_2\text{Al}(\text{Alk})_2]$  which act as the active sites precursors, as do the ion-pairs  $[\text{L}^{\text{iPr}}\text{Fe}^{\text{II}}(\mu\text{-Me})_2\text{AlMe}_2]^+[\text{MeMAO}]^-$  formed upon the interaction of bis(imino)pyridine iron complexes with MAO. In the former structures, reduced bis(imino)pyridine ligand ( $\text{L}^{\text{iPr}(-)}$ ) plays the part of the counteranion (instead of  $\text{MeMAO}^-$  in the latter one), thus giving the catalytically active iron(II) sites. Both types of active sites display comparable ethylene polymerization activities, leading to linear polyethylenes with broad MWDs.

It was shown by Barabanov and co-workers that two types of active sites are present in the systems  $\text{LFeCl}_2/\text{MAO}$  and  $\text{LFeCl}_2/\text{Al}(i\text{Bu})_3$ : the more active (and unstable) sites operating at the early stage of polymerization and giving low-MW PE are transformed into the less active but more stable sites responsible for the higher MW fraction of PE.<sup>15</sup> We presume that the more active sites are intermediates of the type **3**, **6**, and **8**, depending on the activators used. The less active sites can be EPR-active iron species displaying the  $g = 2.08$  peak, formed upon degradation of the initial **3**, **6**, or **8**. The coexistence of (at least) two types of intermediates accounts for the observed multisite nature of the catalyst systems.

## Experimental Section

**General Experimental Details.** All operations were carried out under dry argon by standard Schlenk techniques.

Methylalumoxane (MAO), commercial sample, was purchased from Crompton as a toluene solution (total Al content 1.8 M, Al as  $\text{AlMe}_3 \approx 0.5$  M). For the NMR experiments, PMAO (or PMAO(50)) with a total Al content of 40 wt % and 1–2 mol % of Al as  $\text{AlMe}_3$  was obtained as a solid product by removal of the solvent in vacuo at 50 °C from the commercial MAO. For polymerization experiments, PMAO(20) with a total Al content of 40 wt % and ca. 5 mol % of Al as  $\text{AlMe}_3$  was obtained as a solid product by removal of the solvent in vacuo at 20 °C from the commercial MAO.

Complexes **1**,  $\text{L}^{\text{iPr}}\text{FeCl}$ , and  $\text{L}^{\text{iPr}}\text{FeMe}$  were synthesized as described.<sup>1,29</sup> Toluene- $d_8$  was dried over molecular sieves (4 Å), purified by refluxing over sodium, distilled in dry argon, and stored under argon.  $\text{AlMe}_3$  was purchased from Aldrich and diluted with toluene- $d_8$  (to obtain 0.33–0.1 M solutions).  $\text{Al}(i\text{Bu})_3$  (Aldrich) was purchased as 1 M toluene solution and used as received.  $^1\text{H}$  NMR spectra were recorded at 400.130, on a Bruker Avance-400 MHz NMR spectrometer, using standard 5 mm o.d. glass NMR tubes. The species studied were paramagnetic, with  $^1\text{H}$  NMR shifts strongly depending on the temperature, so the NMR data (see below) are normally presented for two different temperatures.

EPR spectra were measured on a Bruker ER200D spectrometer, 9.4 GHz, in either 5 mm o.d. glass tubes or 4 mm o.d. quartz tubes at room temperature and 77 K.

**Preparation of NMR and EPR Samples.** NMR and EPR samples were prepared as follows: calculated quantities of the iron complexes (generally 1.7–3.3  $\mu\text{mol}$ ) and, if necessary, PMAO or  $\text{B}(\text{C}_6\text{F}_5)_3$  were weighed in the glovebox and placed in the tube, and the tube was closed with a septum stopper. Further addition of toluene- $d_8$ ,  $\text{AlMe}_3$ , or  $\text{Al}(i\text{Bu})_3$  (to achieve the overall volume of 0.5–0.6 mL) was performed outside the glovebox using gas-tight microsyringes in the flow of argon upon appropriate cooling. NMR data of the complexes are summarized in Table 1.

**Ethylene Polymerization Procedure.** Polymerization was performed in a steel 1 L autoclave. The catalyst ( $2.0 \times 10^{-6}$  mol) was introduced into the autoclave in a vacuum-sealed glass ampule. The reactor was evacuated at 80 °C, cooled to 20 °C, and charged with the solution of appropriate cocatalyst in toluene (100 mL). After setting up the polymerization temperature (35

°C) and ethylene pressure (5 bar), the reaction was started by breaking off the ampule with the complex. During polymerization, ethylene pressure, stirring speed, and temperature were maintained constant. After 20 min, the reactor was vented and the polymer was isolated by filtration and dried to constant weight at ambient temperature.

**Polymers MM and MWD Measurements.** Weight-average ( $M_w$ ) and number-average ( $M_n$ ) molecular weights and molecular

weight distributions ( $M_w/M_n$ ) were obtained by the GPC method with a Waters-150 at 150 °C with trichlorobenzene as a solvent.

**Acknowledgment.** This work was supported by the Russian Foundation for Basic Research (grant no. 09-03-00485). The authors are grateful to Dr. L. G. Echevskaya and Dr. M. A. Matsko for the GPC measurements.

OM8010905